7-2002

Propagation of Detonation Waves in Tubes Split from a PDE Thrust Tube

August J. Rolling
Air Force Institute of Technology

Paul I. King
Air Force Institute of Technology

Fred R. Schauer
Air Force Research Laboratory

AIAA 2002-3714
Propagation of Detonation Waves in Tubes Split from a PDE Thrust Tube

August J. Rolling and Paul I. King
Department of Aeronautics and Astronautics
Air Force Institute of Technology
Wright-Patterson AFB, OH 45433

Fred R. Schauer
Air Force Research Laboratory
Propulsion Research and Testing Section
Wright-Patterson AFB, OH 45433

38th AIAA/ASME/SAE/ASEE
Joint Propulsion Conference and Exhibit
7-10 July 2002
Indianapolis, Indiana

PROPAGATION OF DETONATION WAVES IN TUBES SPLIT FROM A PDE THRUST TUBE

August J. Rolling * and Paul I. King †
Department of Aeronautics and Astronautics
Air Force Institute of Technology
WPAFB, OH 45433

Fred R. Schauer ‡
Air Force Research Laboratory
Propulsion Research and Testing Section
WPAFB, OH 45433

Abstract

A Pulse Detonation Engine (PDE) combusts a fuel air mixture through detonation. Existing designs require spark plugs in each separate thrust tube to ignite premixed reactants. A single thrust tube could require the spark plug to fire hundreds of times per second for long durations. This paper reports on the use of a continuously propagating detonation wave as both a thrust producer and a single ignition source for a multi-tube system. The goal was to minimize ignition complexity and increase reliability by limiting the number of ignition sources. The work includes a systematic investigation of single tube geometric effects on detonations. These results were subsequently used to further examine conditions for splitting detonations, i.e., the division of a detonation wave into two separate detonation waves. Finally, a dual thrust tube system was built and tested that successfully employed a single spark to initiate detonation in separate thrust tubes.

Introduction

A Pulse Detonation Engine, PDE, is a tube filled with a combustible mixture, closed at one end, and ignited. The high pressure behind the detonation wave at the closed end of the tube and the rapid expulsion of products from the open end produces thrust. Fig. 1 shows the test PDE, which is located at Wright-Patterson AFB. The photograph shows four thrust tubes, but testing for this project used one or two tubes. The expelled exhaust products visible in Fig. 1 are a result of detonation combustion.

Due to the high temperatures and harsh vibrations, integration of components and systems into a PDE poses major problems, one of which is the ignition system. The use of spark plugs for ignition is convenient for small scale testing at low frequencies, but larger scale testing and practical systems could require frequencies on the order of 100 Hertz for long durations. These requirements and the relative complexity of a multi-tube engine require complex ignition systems that can withstand harsh environments.

The approach taken for this research involved replacing the spark plug ignition with the hot exhaust gases trailing a detonation wave diverted from the main thruster tube. These hot gases in a split tube can than ignite another thrust tube. The work reported here is in three parts. The first includes an investigation of tube geometry on detonation strength. The second part reports on the effect of tube geometry on the ability to split a propagating detonation wave, and the third includes results of a dual thrust tube arrangement ignited by a single ignition source.

Materials and Methods

<u>Research facility</u>

The ability to produce thrust can be explained with the aid of Fig. 2, which shows a PDE cycle. With a fuel air mixture injected into the thrust tube, the mixture is ignited and quickly transitioned to a propagating detonation wave. Compressed air then forces out remaining products and separates hot products from fresh reactants. This cycle repeats at a desired frequency. An attractive feature of this cycle is that conventional automotive engine valving can be used.

The main components of the research facility are illustrated in Fig. 3. All points of operation are monitored and controlled virtually with National Instruments LabVIEW™ software. Metered compressed air and fuel

*Capt, USAF, Master's student
†Associate Professor, senior member
‡Research Engineer, member

The views expressed in this article are those of the authors and do not reflect the official policy or position of the United States Air Force, the Department of Defense, or the U.S. Government.

enter the engine and the reservoir pressure is monitored. An upstream orifice provides a choke point and maintenance of mass flow rate. A General Motors Quad 4, Dual Overhead Cam (DOHC) cylinder head, commonly used in the Pontiac Grand Am, provides the necessary valving. The engine is mounted to a damped thrust stand that measures axial thrust. The engine can run up to four thrust tubes simultaneously. The entire system is controlled and monitored remotely including: lubrication, valve drive speed, fuel flow, main combustion air flow, purge air flow, timing, ignition delay (time of spark within detonation phase of PDE cycle), low and high frequency data collection, and automatic shutdown in the event of a critical system failure. Certain key parameters were varied to optimize each configuration. For single and split tubes, tube fill fraction was 1.0 (amount of total volume filled during fill and purge phases), equivalence ratio (φ) was 1.0, frequency was 20 Hz and ignition delay was 5 ms. A complete description of the test facility is given by Schauer et al.[1]

Data acquisition

The data acquisition software allows a preview of wave speeds, thrust, and pressures, and shows each transducer pressure-time trace.[2] This gives immediate feedback on the health of the acquisition system while offering a first look at experimental results. The program uses a bottom constant threshold method for determining wave speeds. The bottom method uses the first crossing of a pressure trace over a threshold to signal detonation passage. The threshold is held constant, ignoring thermal drift. This method provides quick feedback for on-the-fly adjustments.

The data acquisition system acquired data at 4 million data points per second. The pressure transducers were PCB Piezotronics Inc. model 102M232, series 111A general-purpose miniature sensors (PFS 2000). These transducers have pressure ranges from vacuum to 3000 psi. The sensor useable frequency range is between 20 kHz and 30 kHz with a resonant frequency of 130 kHz.

Detonation initiation

In order for a pulse detonation engine (PDE) to function properly, deflagration to detonation transition (DDT) must occur. Additionally, it should occur quickly and in a short space. The failure of V-1 buzz bomb to achieve detonation demonstrated the difficulty of achieving those conditions.[3] Several DDT tripping geometries have been shown to induce detonations.[4,5,6] A Shelkin spiral, for example, generates acoustic reflections that interact and form hot spots. These hot spots promote detonation transition. Such a spiral may produce consistent detonations in a short distance. In this work, about 5 pipe diameters were required axially for a 2-inch diameter pipe.

Detonation Criteria

A 1-D and ZND analysis verified Soloukhin's[7] data for stoichiometric H_2 and air. Therefore, those values were the criteria for confirmation of detonation waves. Wave speeds and pressures were measured at several points along any test configuration, and any wave with speed of 1968 m/s was considered a possible detonation wave. A second necessary condition came from the pressure ratio of 15.62 across the detonation wave. For a 14.7 psi (101.3 kPa) baseline pressure, the P_2 pressure should be at least 229.6 psi (1.583 MPa) following the passage of a detonation wave.

Experimental configurations

In order to make informed design decisions, a better understanding of geometric effect on detonation physics was required. To expedite the experiment and because the existing engine hardware mates to two-inch pipe, commercial two-inch pipe was used. A second, ¾ inch pipe served as a split tube. This latter diameter was selected to minimize fuel consumption while being of sufficient diameter to contain at least one detonation cell width, which for stoichiometric H_2 and air is 15 mm.

Single tube configurations

One objective was to identify configurations that would promote the propagation of a detonation wave through a split. Candidate configurations included converging, diverging, and 90-degree turn geometries. Additionally, downstream diameter reduction effects were examined via an abrupt 2-inch to 1 ½ inch reduction and a gradual transition reducer.

Figure 4 shows the engine and tubes common to all configurations and containing transducers 1 and 2. The detonation wave propagates from left to right. Pressure transducer 1 was mounted in the engine block in the head of cylinder 1. A cutaway view reveals the 12-inch DDT spiral. Pressure transducers 3 and 4 were mounted in either a two-inch tube (shown in figure) or a ¾-inch tube. These transducers measured the wave speed to ensure the speed entering the experimental attachment was at upper Chapman-Jouguet value.

One set of experimental attachments is shown in Fig. 5. Configurations a, b, e and f represent a progression in tube extension. Configurations c-g and d-h are abrupt and gradual reductions, respectively.

Figure 6 shows step-up transitions, with and without end transitions; b-c are gradual and d-e are abrupt. These geometries modeled split tube to thrust tube divergence.

Figure 7 shows models for investigating turns that would be implemented in a multi-tube thruster. Flow from the engine for configurations a, b, c and d originate in a two-inch tube, while for e, f and g, flow originates in a 3/4 –inch tube. Configuration b was for examining the effect of downstream geometry; c-d and e-f were step down and step up transitions, respectively. (CFD predicted that step up expansions would dissipate a detonation.[8])

Split tube configurations

A second investigation was to attempt a detonation split. Again, only commercially available parts were used, limiting designs to 90-degree splits via tees, and 45-degree splits via wyes.

Figure 8 shows splits with tees. Theses geometries seemed to offer the least potential for a split detonation (due to the abrupt 90-degree turn), but less complexity for scaling up. Configurations a-d had splits with continuing tube diameter, while e-h had splits followed by step down diameters to attempt to encourage the detonation into the split tubes (containing transducers 7 and 8). Configurations b, d, and h contained end nozzles; e-f were for comparison of abrupt and gradual split, respectively. A similar logic was applied to the wye configurations of Fig. 9.

The use of capped ends to create high downstream pressure conditions was tested with the configurations shown in Fig. 10.

Dual thrust tube - single ignition source

Figure 11 shows the configuration tested to obtain dual-tube detonation from a single spark source. The two thrust tubes furnish one section of a multiple thrust tube array.

An important challenge in testing this configuration was ignition timing. Due to the fixed valve phasing, the window of opportunity to fire either spark was limited. Figure 12 shows the offset of cycles between the first and the third tube positions. The thrust tubes were numbered according to engine block location. These positions were chosen on the engine block because the valve position is only 90-degrees out of phase. (Typical engine spark plug firing order was 1-3-2-4 in 90 degree increments.) To fire spark 1, the cycle had to be within the burn cycle of tube 1. Additionally, tube 3 had to complete the fill cycle before the flame front completed traversing the crossover tube. Dependent on the amount of time for ignition, DDT, and the detonation to travel through the crossover to tube 3, the ignition time for tube 3 was typically a few milliseconds after spark plug 1 fired.

The firing window was initially limited to the beginning of the tube 3 burn cycle. During actual testing, slightly more aggressive earlier firings were attempted, while avoiding backfiring. Table 1 shows ignition delay times based on run frequency. The delay times were measured from the beginning of the corresponding cylinder burn phase. Here, the effect of ignition delay on performance was systematically tested by varying ignition delay and measuring resulting thrust and wave speeds.

Table 1 Ignition delay time vs. frequency

	Frequency (Hz)	20.00	30.00	40.00
	Cycle Time (ms)	50.00	33.33	25.00
Spark Plug 1	min delay (ms)	12.50	8.33	6.30
	max delay (ms)	16.70	11.11	8.33
Spark Plug 3	min delay (ms)	0.00	0.00	0.00
	max delay (ms)	4.20	2.80	2.10

A narrow window is available for the firing sequence to be successful. For example, while running at 30 Hz, the firing window for spark plug 1 is only 2.8 ms. Though the configuration is intended to work while firing only spark 1, a thorough matrix was investigated consisting of firing spark 1 only, spark 3 only, and both sparks.

Results and Analysis

Data post processing

In-house developed software was used for post processing.[9] It allows the user to choose between a top, middle, and bottom method for determining wave speed. Each method establishes the time of detonation passage. The bottom method is based on a first crossing of a chosen threshold. The top method is based on the peak pressure, and the middle method is based on these points and slopes. A sensitivity analysis of method vs. threshold was conducted. For user-selected thresholds of 50, 100, 150, and 200 psi, the top and middle method independently maintained results within 3%. The bottom method was greatly dependent on chosen threshold, varying by more than 10% in some cases. Since middle method results are typically published, that method with a threshold of 100 psi was used for post-processing all data. Additionally, a linear regression method was employed to account for thermal drift.

Pressure uncertainty is difficult to quantify. The pressure across a detonation cell can range from 16.25 atm. to 116.5 atm.[6] Since a single cell is slightly shorter than one inch, there are very large pressure gradients. Unfortunately, the pressure transducer diameter was 3/8 inch; and thus these large pressure gradients were spatially averaged over a surface length similar to the cell size. Even though the sensor may be accurate within 10 psi, the physics of the detonation cell can inherently produce much larger error. To reduce uncertainties, each configuration was run at least twice. Each run was post-processed separately, and the data were compared. If there was a discrepancy between runs, the average of the individual detonation wave speeds was used. Data were usually acquired over a 0.5 s period. Since the majority of tests were run at 20 Hz, 10 detonation peaks were thus normally acquired.

A percent of CJ value was calculated for each average wave speed using the relationship, (wavespeed/1968 –1) x 100%. Once this value was calculated, the quality of the wave speed was determined and denoted as shown in Table 2. The symbols in Table 2 were placed directly on the test configuration schematic. Additionally, for any average pressure that drops below the expected state 2 ZND value of 229 psig, the pressure transducer was circled. Therefore, if a wave speed showed out of range and there was a circle around either one or both corresponding transducer numbers, the system was not detonating.

Table 2 Classification by %CJ

Wave speed (m/s)		% CJ		Qualification	Symbol
low	high	low	high		
2086.1	3000.0	6%	52%	over-driven	
1869.6	2066.4	-5%	5%	excellent	
1672.8	1869.6	-15%	-5%	good	
50.0	1672.8	-97%	-15%	bad	

Single Tube Results

The results for the first single tube test are illustrated in Fig. 13. The high wave speed and pressures shown in configurations a and b signify a transition phenomenon. Little effect on wave speed occurred when applying the step transition configuration c, versus the gradual transition in d. This was also the case when the ¾-inch section was attached, g vs. h. The reducer on configuration f also failed to affect the wave speeds seen in e. It should be noted that though the wave speed had decelerated slightly in e, this does not discount that detonations were occurring. Rather, this only signals a degradation in average wave speed that is not desirable in system design. From this test matrix, it seemed that converging configurations do not provide a tangible benefit for increasing wave speed.

Figure 14 shows results for step up transition. The baseline configuration (a) could have strong detonations. CFD results predicted that the size of the expansion was too large for the detonation to maintain strength.[8] Results in Fig. 14 b,c,d and e confirmed this.

The latter four case results shed light onto desired geometries, however. Although a ¾ inch to 2-inch expansion was too large, the gradual transition via the (reversed) reducer maintained a relatively high pressure. The pressure was at least 3 times larger in the expanded sections of b and c than in the same sections of d and e. A tripping device in the 2-inch diameter sections of configurations b or c would cause quicker transition than in d or e.

Figure 15 shows the effect of turning detonations through 90-degrees. Unfortunately, the commercially available stainless 90's had limited turning radii. (Other pipe materials like PVC have street 90's with larger turning radii.) The wave speed symbols between transducers 4 and 5 were omitted. This was due to the slightly larger inherent error when measuring around the bend.

The wave speeds and pressures throughout configurations a and b were consistent with CJ detonations. The converging bends of c and d reduced pressure and wave speed. The expanding bends of e and f also reduced pressure and wave speed. Since the horizontal segment in g did not achieve detonation wave speeds, it was not possible to qualify the effect of a ¾ inch 90-degree turn on a detonating structure. The effect of downstream geometry was apparent comparing the excellent wave speed in the horizontal sections of e and f to the bad wave speed in the same section of g. Both e and f were able to achieve CJ wave speeds between 3 and 4, while g was 40% lower.

Certain trends were noted by comparing configurations throughout the results of single tube configurations. The wave speeds in the turned tubes of Fig. 15 a and b were within 5% of expected CJ speeds as opposed to the lower speeds of the straight tubes in Fig. 13 e and f. This indicates detonation strengthening around a bend, possibly due to shock reflections.

Summary of single tube results

- Converging configurations decreased wave speed
- ¾ inch to two-inch step up was too large - decreased wave speed
- Gradual divergence maintains higher pressure than step divergence
- CJ detonations through like sized bends maintained strength
- Downstream geometries affected upstream wave speeds

Split tube results

Figure 16 shows the results of tee configurations on wave speed and pressure. Only configurations b and e achieved detonation in split tubes. A comparison of a-b and g-h indicates speed in the opposing tube increased with a nozzle. This could have been due to forcing mass flow, hence more fuel and air, into the split tube during the fill cycle. The abrupt step-downs of e performed much better than the gradual transitions of f. Possibly this is due to stronger shock interaction due to reflections off the interior bushing wall.

Figure 17 shows the results of detonating through wyes. The step convergent configuration e met the desired objective to split a detonation. As with the successful tee configuration, this step transition also had higher wave speeds in the splits than the gradual transition configuration f. This pointed to some interesting physics that was not predicted by the single tube step configuration results. Recall that Fig. 13 configurations g and h both retarded the wave speeds regardless of step or gradual transition. Clearly, the downstream geometry, split, encouraged the higher speeds in the step configurations of Fig.'s 17 e and f.

Figure 18 shows the results of cap geometries. Configuration c shows that high wave speeds were not encouraged by the 45-degree turn. By comparing b and c, the upstream wave speed was increased with a 45- degree turn versus an abrupt 90-degree. This confirmed the earlier finding that downstream geometries do affect upstream wave speeds. Configuration a showed a degradation in wave speed. Also, the expected higher pressure rise did not occur, possibly due to a lack of a reflected detonation wave.

An examination of the effect of increased fill fraction was conducted with the tees and wyes of Fig.'s 8 a-b and 9 a-b, respectively, at a fill fraction of 1.25.

Figure 19 shows the effect of increased fill fraction. Here the higher fill fraction and the reducer increased wave speeds in critical areas of the configuration. Figure 19 shows that the addition of a reducer is more effective than an increased fill fraction (c.f., Fig. 19a-b-e, and c-g-d). Although the reducer increases weight, the higher fill fraction increases fuel consumption by 25%.

<u>Summary of split tube results</u>

- Double convergent tee and wye configurations split detonations
- Step transitions performed better than gradual in split configurations
- Nozzles on splits increased wave speeds in opposing tubes
- Downstream geometry affected upstream wave speed
- Increased fill fraction increased wave speeds
- Convergent reducer increased upstream wave speed
- Reducer benefits outperformed 125% fill fraction gains

<u>Dual thrust tube – single ignition source results</u>

The configuration shown in Fig. 20 achieved detonations in two thrust tubes using a single ignition source. The thrust tubes are numbered 1 and 3 corresponding to their cylinder position on the engine block. The ¾ inch diameter stainless crossover tube is mated to each 2-inch diameter thrust tube via a standard 2-inch to ¾ inch tee.

The spark plug in tube 1 was the only ignition source. After ignition, a 12-inch spiral accelerated DDT before reaching the tee. At the tee, part of the detonation wave continued down tube 1. The exact physical state of combustion, i.e., whether detonation or deflagration, at the crossover entrance could not be determined without more complicated instrumentation. However, the wave speeds through the crossover accelerated to more than 10% above the Chapman Jouguet detonation speed. This fact combined with the high pressure reading near the crossover entrance, transducer 3, Fig. 21, implied a continuation of detonation, or at least a second rapid DDT event.

The geometric divergence into tube 3 quenched any detonation formed in the crossover tube by dissipating the shocks. The lower pressure at the first transducer in tube 3, transducer 5, Fig. 21 evidenced this phenomenon. However, the premixed reactants in tube 3 coupled with these weaker shocks readily recombined into a full detonation when confronted with a 16-inch DDT spiral. Thus another, arguably the third, deflagration to detonation transition mechanism occurred. Results show that downstream of the second spiral, the reaction in tube 3 was a detonation.

The high wave speed through the crossover represent either a strong detonation or a point along the transition path such as the von Neumann spike. The first consideration is the position along the Rankine Hugoniot curve. Because the pressure has dropped considerable by transducer 4, this cannot represent a strong detonation. Therefore, this high wave speed occurs because of the transition process.

One explanation is that Kuo's "explosion in the explosion" occurred downstream of pressure transducer 3.[10] Then transducer 3 would have sensed the retonation wave and transducer 4 would have sensed the superdetonation wave. This would have definitely lowered the time and increased wave speed. Since transducer 4 was not reading ZND state 2 pressures, however, another event was probably happening here. Clearly, the combustion process is still coupled with shocks since the pressure was over 10 times atmospheric at transducer 4 and tube 3 ignited. The crossover tube captured a transition mechanism, but without more sophisticated instrumentation, it was not possible to determine that mechanism's point along the transition path.

The following pressure traces correspond to these test conditions: fill fraction = 1.0, equivalence ratio, $\varphi = 1.0$, frequency = 30 Hz, and ignition delay = 9.0 ms for spark plug 1. The data collected covers a 0.5 s interval, corresponding to 15 detonation waves.

The results of this test were high average wave speeds. The pressures measured at downstream locations on the thrust tubes were at or above those predicted from ZND analysis. The detonation speeds were within 5 % of CJ speeds at all measured locations. The wave speeds between transducers 3 and 4 were above CJ wave speed. The achievement of these higher wave speeds was desirable from a thrust perspective, but not necessarily in the crossover tube.

Regardless of the actual physical mechanism occurring in the crossover tube, two things are apparent. This configuration achieved the desired goal, but exact detonation mitosis did not occur. The offspring detonation in the crossover tube did not carry the same physical characteristics of the parent wave. There is room to improve the process and maintain full and steady detonation propagation throughout the entire process.

An examination of pressure traces for the first run provides valuable information. The traces at transducers 1, 2, 6, 7, and 8 indicate propagating detonation waves. The traces for the crossover tube transducers and the first transducer in tube 3 are provided. Figure 22 shows that detonations occurred inside the crossover tube at transducer 3. Figure 23 shows that the detonations did not propagate through the entire crossover tube.

Although the pressure trace in Fig 23 shows that von Neumann pressures did not occur, there was a sharp pressure rise. This pressure rise at transducer 4 suggests a shock wave followed by a combustion front, the first step in the DDT mechanism. Though this is not detonation, it shows shock interaction that is clearly not present at transducer 5. Figure 24 shows the gradual pressure rise that occurred near the entrance of tube 3 prior to DDT. This represents deflagration.

Timing is critical to success of this technology. One can gain a full sense of the timing from Fig. 25 which shows the key events in milliseconds (ms) for the successful dual thrust tube configuration. Only pressure transducers 1 and 8 are represented because the total elapsed time between an event at the first transducer and the last is 1.11 ms.

Summary of dual-tube detonation

- A single spark initiated detonations in tubes 1 and 3 at 30 Hz
- Timing, frequency and ignition delay, is critical for success
- Timing is hardware dependant especially on crossover length.
- Crossover physics may require instrumentation that is more sophisticated.

Conclusions

A dual-tube apparatus was tested and proved the ability to use a single ignition source to produce thrust in a dual detonation tube configuration. The initial phases of testing showed that varying geometry affected wave speed and peak pressure. Whether this happened due to the initial conditions of the reactants just after the fill phase or because of detonation physics requires further investigation.

Some additional observations were made. Either the nozzles provided an increase in wave speed or no detrimental effect on the wave speed was noted. A higher fill fraction had a positive impact on wave speed, but would probably be cost prohibitive, and less efficient. The diameter ratio of all expansion configurations was too large. Timing was critical in the success of the dual detonation configuration. This was largely due to the length of the crossover tube. Finally, more extensive instrumentation and testing are required to understand certain aspects of the physics, especially to make a successful reflector trip device.

Acknowledgements

This work was sponsored and funded by the Air Force Research Laboratory Propulsion Directorate, Turbine Engine Division, Combustion Sciences Branch, Wright-Patterson AFB, Ohio. The authors also wish to thank Dr. John Hoke and Royce Bradley for their assistance in the experimental work and interpretation of findings, and to Mr. Jeff Stutrud who wrote the data acquisition software. Additional gratitude is owed to Dr. Vish Katta for his CFD work on deflagration/detonation, and Mr. Jason Parker for his contributions on data analysis.

References

1. Schauer, F.R., Stutrud, J., Bradley, R. and Katta, V.R., "AFRL/PRSC Pulse Detonation Engine Program," invited paper at 12th PERC Symposium, Ohio Aerospace Institute, Cleveland, OH, 26-27 Oct. 2000.
2. Stutrud, J., *Tutorial on the Online Wave Speed Program VI,* Unpublished Report for Air Force Research Laboratory, Propulsion Research and Testing Section, Wright-Patterson AFB OH, 4 December 2001.
3. Oppenheim, A.K., "Research and Development of Impulsive Ducts in Germany," *B.I.O.S.* Final Report No. 1777, Item No. 266, England, (1949).
4. Shelkin, K.I. *Soviet Journal of Technical Physics*, Vol. 10 page 823-827, 1940.
5. Schauer, F.R., Bradley, R., Katta, V.R. and Hoke, J., "Detonation Initiation and Performance in Complex Hydrocarbon Fueled Pulsed Detonation Engines," 50th JANNAF Propulsion Meeting, Salt Lake City UT, 11-13 July 2001.
6. Katta, V.R., Chin, L.P. and Schauer, F.R., "Numerical Studies on Cellular Detonation Wave Subjected to Sudden Expansion," Proceedings of the 17th International Colloquium on the Dynamics of Explosions and Reactive Systems, Heidelberg, Germany, 1999.
7. Soloukhin, R.I. *Shock Waves and Detonations in Gases*. Moscow: Mono Book Corp., 1966.
8. Katta, V.R., Air Force Research Laboratory/ Propulsion Research and Testing Section, Wright-Patterson AFB OH. Personal Interview, January 2002.
9. Parker, J.T. and Schauer, F.R., "Analysis and Compression Algorithms for Megabyte Range PDE Data Sets" presentation to Dayton Cincinnati Aerospace Sciences Symposium, Dayton OH, 7 Mar. 2002.
10. Kuo, K.K. *Principles of Combustion*, New York: John Wiley & Sons, 1986.

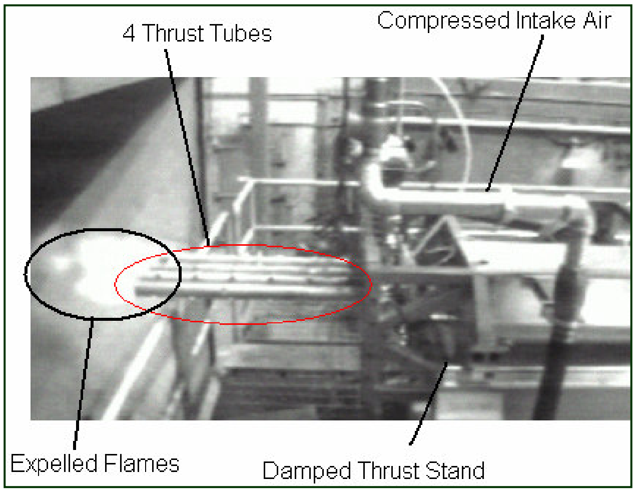

Fig. 1 Building 71 Test Pulse Detonation Engine

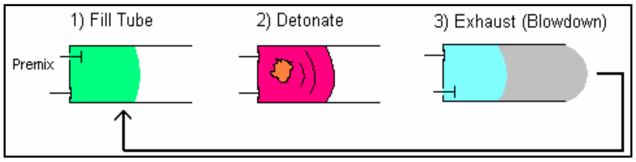

Fig. 2 PDE engine cycle

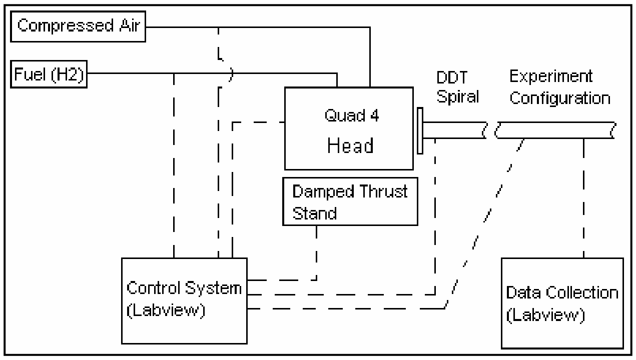

Fig. 3 Schematic of research facility

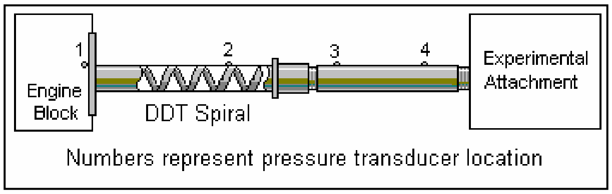

Fig. 4 Baseline test configuration

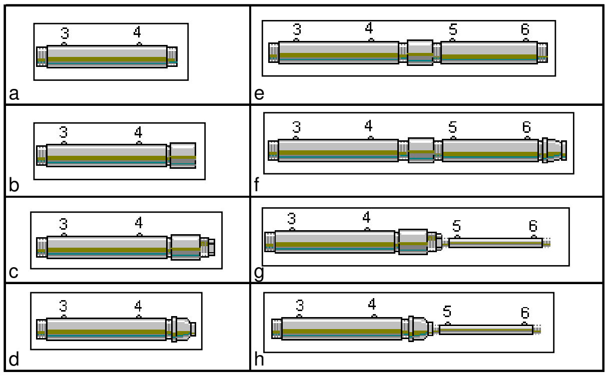

Fig. 5 Axially converging geometries

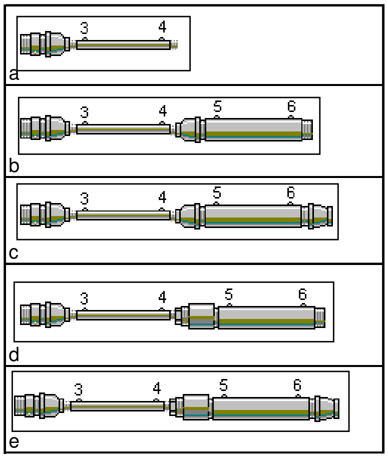

Fig. 6 Axial diverging geometries

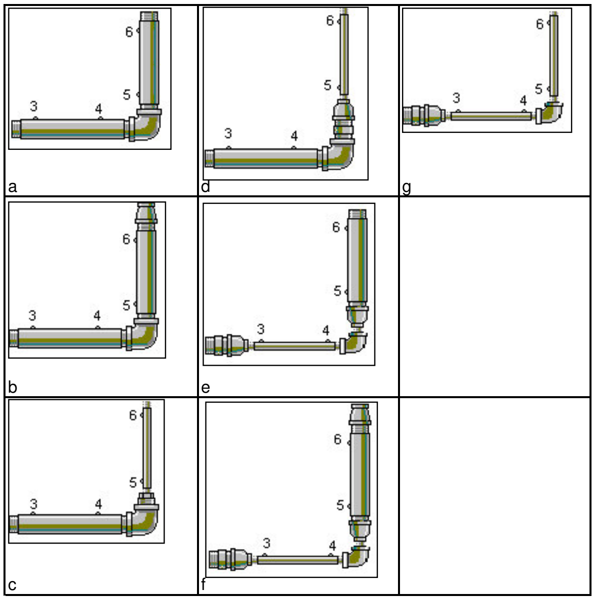

Fig. 7 90-degree turns

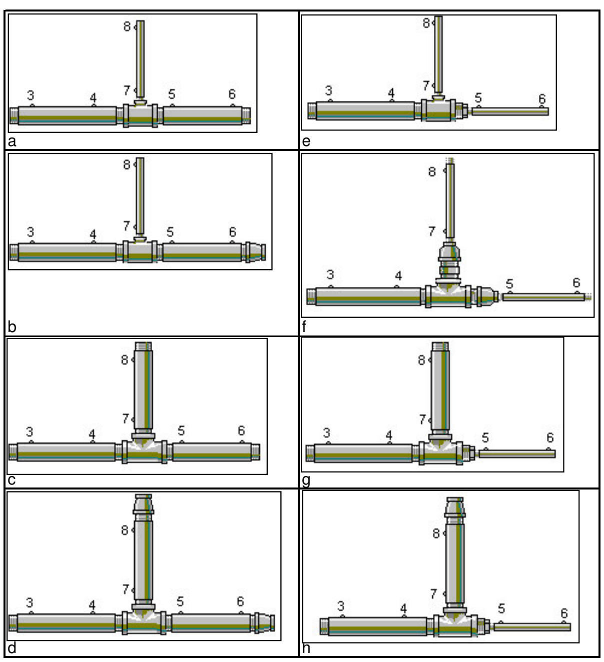

Fig. 8 Tee geometries

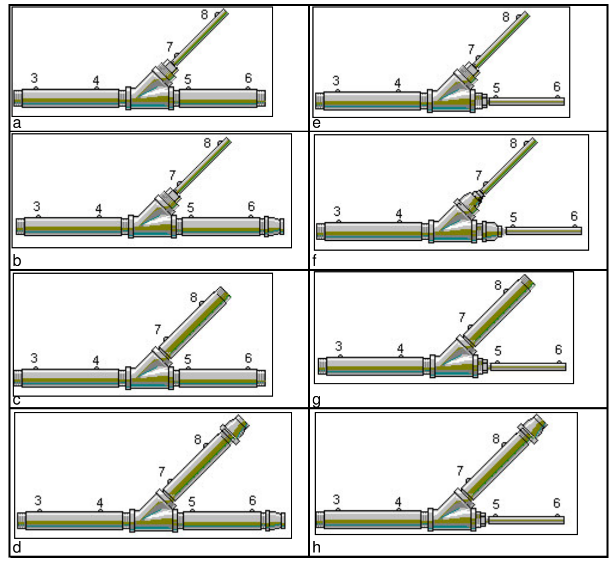

Fig. 9 Wye geometries

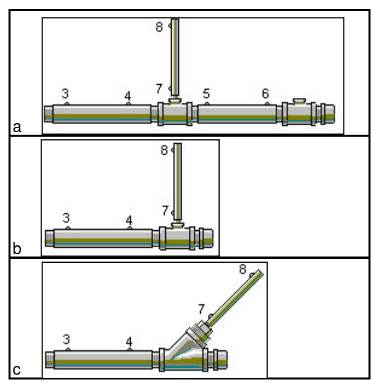

Fig. 10 Capped geometries

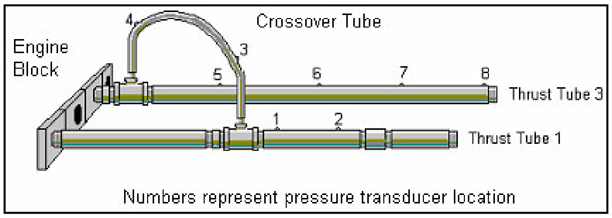

Fig. 11 Dual thrust tube

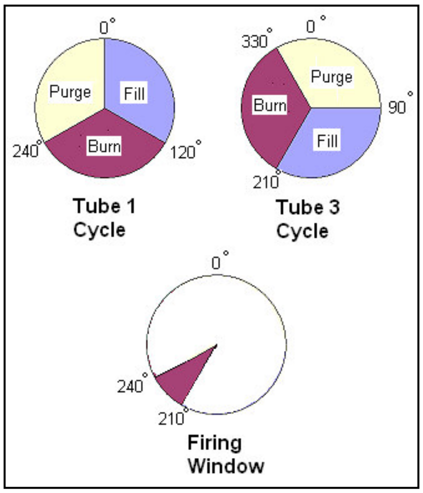

Fig. 12 Cycle diagrams and firing window

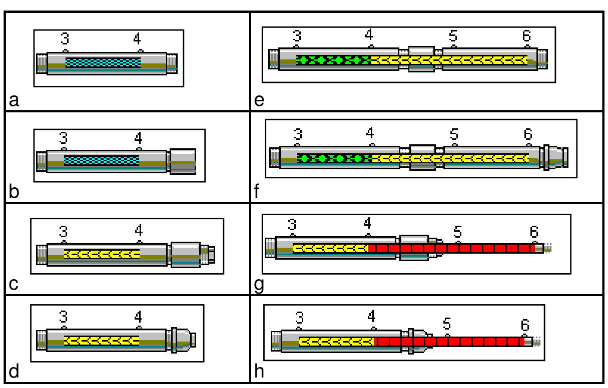

Fig. 13 Results: axial converging

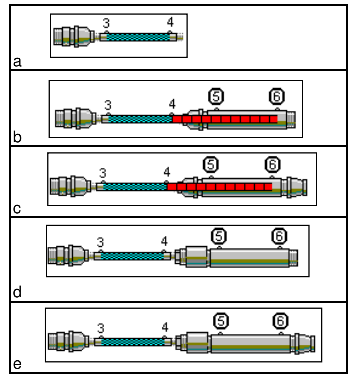

Fig. 14 Results: axial diverging

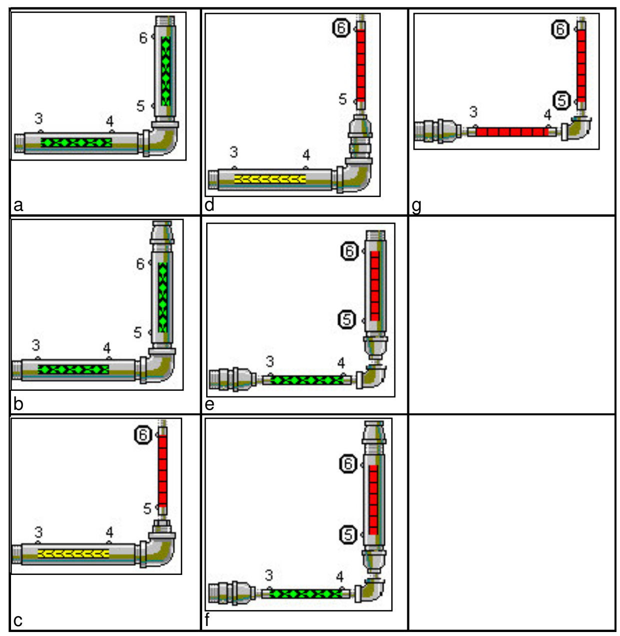

Fig. 15 Results: 90-degree turns

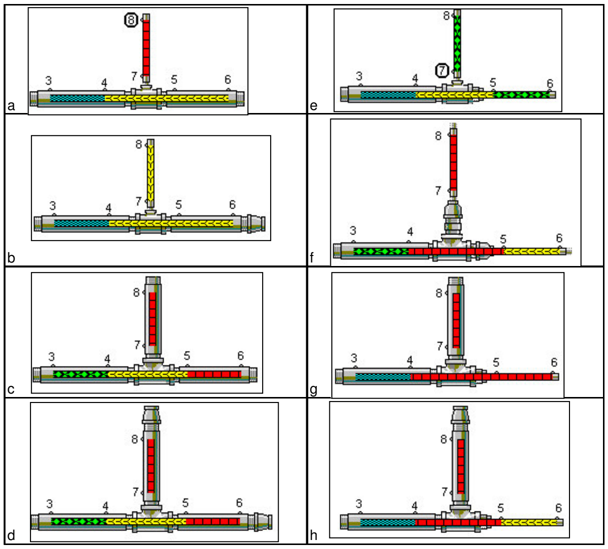
Fig. 16 Results: tees

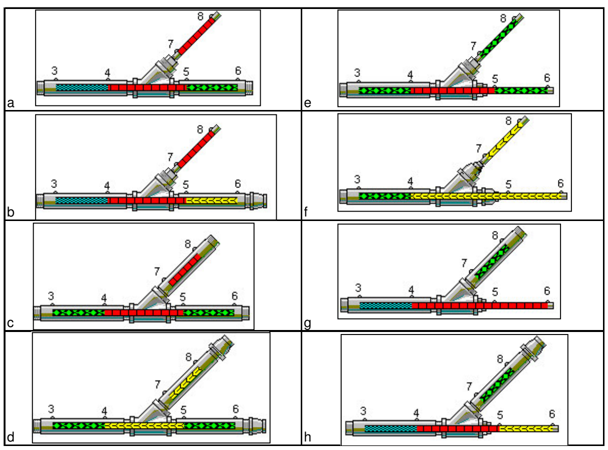
Fig. 17 Results: wyes

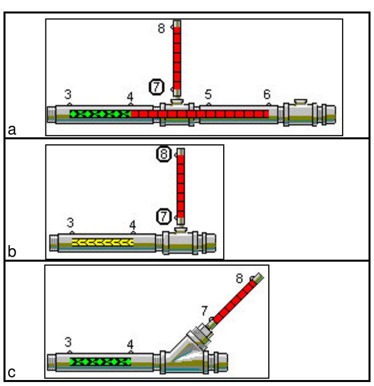
Fig. 18 Results: caps

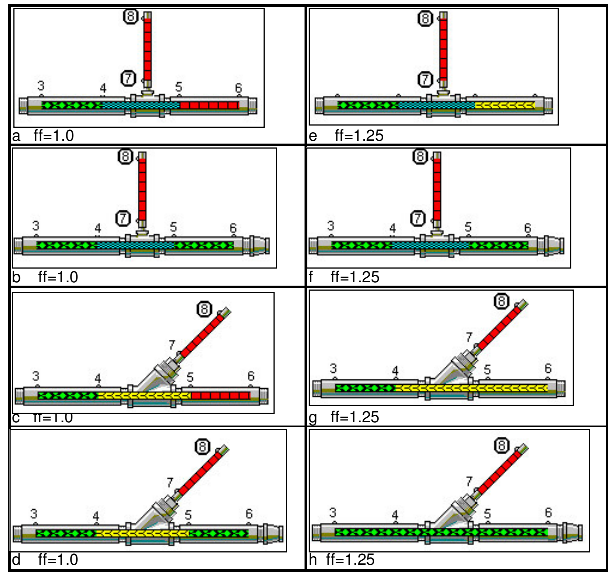

Fig. 19 Fill fraction effects

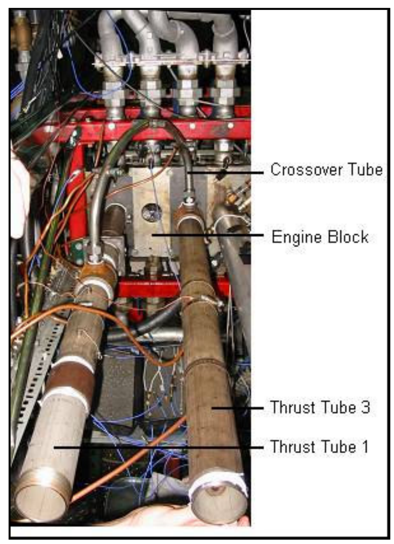

Fig. 20 Single spark, dual detonation configuration

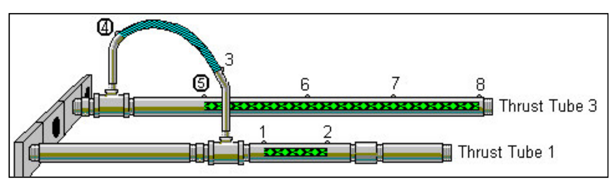

Fig. 21 Dual detonation results

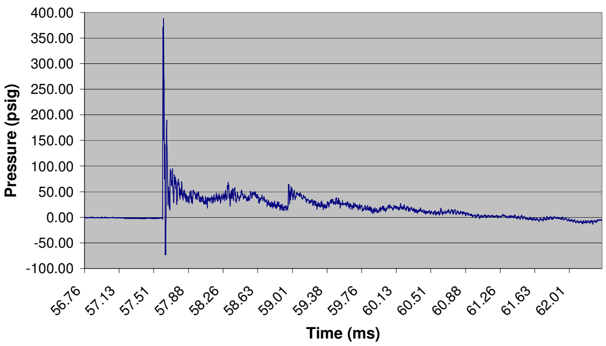

Fig. 22 Dual tube transducer 3 pressure trace

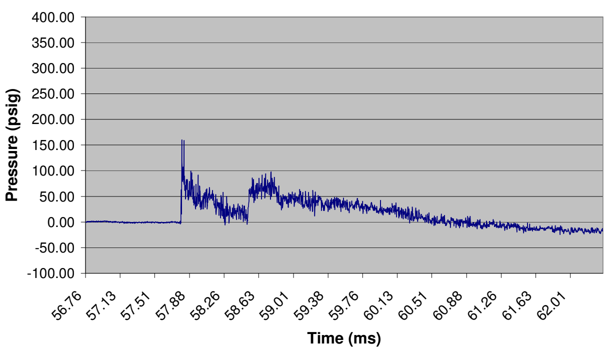

Fig. 23 Dual tube transducer 4 pressure trace

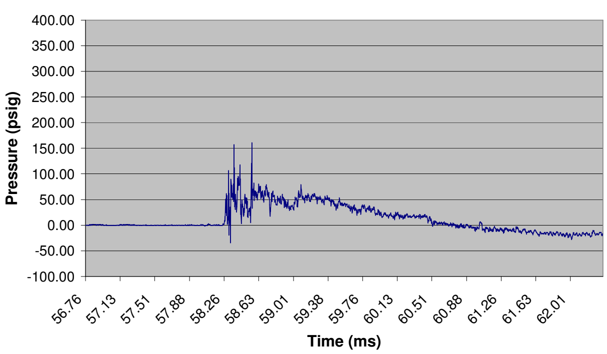

Fig. 24 Dual tube transducer 5 pressure trace

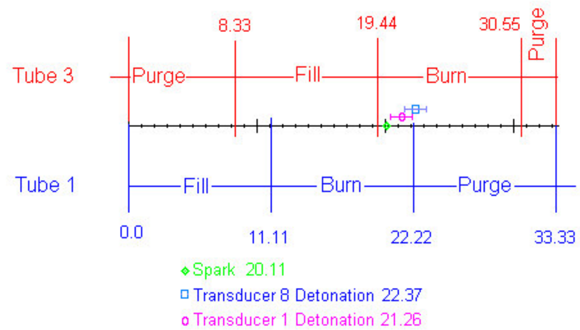

Fig. 25 Dual thrust tube detonation sequence (ms)